Supporting Information

Self-assembled $PrBaCo_2O_{5+\delta}$-$Ba_{0.9}CoO_{3-\delta}$ composite as highly active and durable oxygen electrode for reversible solid oxide cells

Min Zhang,[a] Jiayue Liu,[a] Xinyang Yu,[a] Yang He,[a] Zhihong Du,[a,b] Xianyu Wang,[a] Boyang Fu,[c] Konrad Świerczek,[c] Jianrong Zeng,[d,e] Ligang Wang,[f] Hailei Zhao[a,b,*]

a School of Materials Science and Engineering, University of Science and Technology Beijing, Beijing 100083, China

b Beijing Municipal Key Lab for Advanced Energy Materials and Technologies, Beijing 100083, China

c Faculty of Energy and Fuels, AGH University of Krakow, al. Mickiewicza 30, Krakow 30-059, Poland

d Shanghai Synchrotron Radiation Facility, Shanghai Advanced Research Institute, Chinese Academy of Sciences, Shanghai 201204, China

e Shanghai Institute of Applied Physics, Chinese Academy of Sciences, Shanghai 201800, China

f Beijing Laboratory of New Energy Storage Technology, North China Electric Power University, Beijing, 102206, China

*Corresponding author:

Hailei Zhao, E-mail address: hlzhao@ustb.edu.cn

Supplementary Note 1

The PBC-B9C composite with mass ratio of 8:2 was synthesized by a sol-gel method. First, the Pr_6O_{11} (Aladdin, 99.99%), $Ba(NO_3)_2$ (Sinopharm Chemical, AR), and $Co(NO_3)_2 \cdot 6H_2O$ (Macklin, 99.99%) were dissolved in dilute nitric acid. Then citric acid (Macklin, 99.5%) was added to the solution to complex Pr^{3+} and Co^{3+} with a molar ratio of 2:1, and ethylenediaminetetraacetic acid (Sinopharm Chemical, AR) was used to complex Ba^{2+} at a molar ratio of 1:1. The pH of the mixed solution was adjusted to 5–6 with ammonium hydroxide. The final solution was heated in a water bath to evaporate most of the water and turned into a gel after heating in a drying oven at 80 °C. Then the gel was further heated at 250 °C for self-combustion to obtain fluffy precursors.

Supplementary Note 2

The ECR method was performed to investigate the oxygen surface exchange. First, the PBC-B9C and PBC dense bars with a relative density about 95% were obtained by sintering the pressed green samples at 1150 °C and 1200 °C for 4 h in air, respectively. Then both of the PBC-B9C and PBC bars were polished into the sizes of about 21.0 mm × 5.0 mm × 1.0 mm, which was suitable for calculating the oxygen surface exchange coefficients (k_{ex}). The data were recorded by using a high-precision digital multimeter (Keithley 2100) at the temperature range of 600-800 °C with a step of 50 °C. The testing atmosphere was dynamically switched between 10% O_2/90% N_2 (0.1 atm) and 20% O_2/80% N_2 (0.2 atm) to simulate the oxygen reduction reaction (ORR) and oxygen evolution reaction (OER) processes, respectively. Specifically, the switch from 0.1 atm to 0.2 atm simulated the ORR process, while the reverse switch simulated the OER process. The flow rate of the atmosphere was 200 mL min^{-1}, which was controlled by the gas mass flow controllers (Alicat Scientific). The k_{ex} was fitted by the Matlab program, which is based on the Fick's second law.

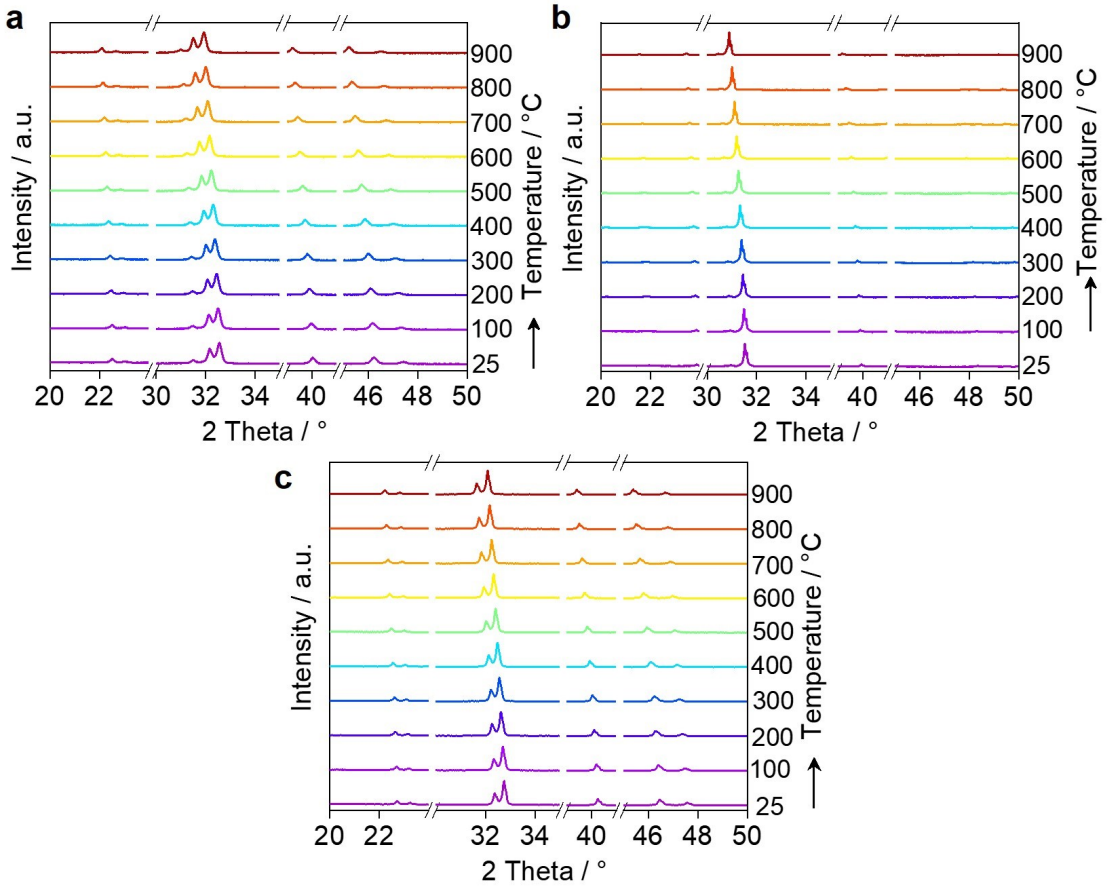

Fig. S1. HT-XRD patterns of PBC-B9C (a), B9C (b) and PBC-B9C (c) samples measured in air

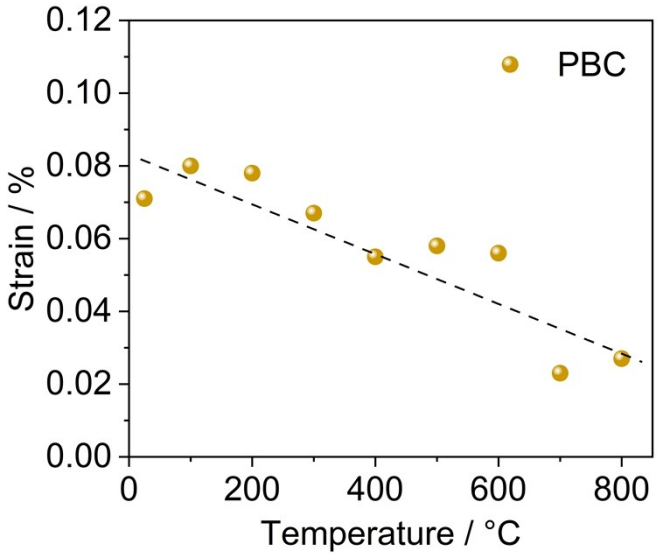

Fig. S2. Calculated microstrain of PBC phase in the PBC-B9C composite at different temperatures, based on high-temperature XRD data (Fig. S1).

Table S1. FWHM trend with different lattice plane of PBC phase in the PBC-B9C composite at different temperatures.*

(hkl)	25 °C	100 °C	300 °C	500 °C	700 °C
(100)	0.151	0.168	0.149	0.147	0.135
(200)	0.210	0.181	0.173	0.158	0.147
(102)	0.187	0.188	0.180	0.173	0.168
(112)	0.185	0.180	0.180	0.166	0.170
(200)	0.217	0.210	0.201	0.177	0.177
(004)	0.252	0.247	0.241	0.203	0.187
(212)	0.223	0.229	0.222	0.206	0.195
(114)	0.238	0.234	0.233	0.213	0.198
(220)	0.240	0.252	0.229	0.237	0.210
(204)	0.265	0.233	0.267	0.238	0.215
(310)	0.498	0.489	0.355	0.432	0.274

*The FWHM of all diffraction peaks across the measured 2θ range exhibits a general decreasing trend with temperature. This uniform narrowing indicates a homogeneous reduction in microstrain throughout the crystal lattice with temperature.

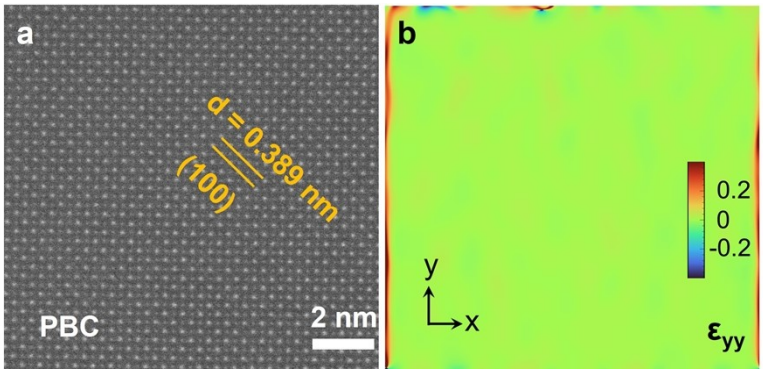

Fig. S3. High-resolution STEM image (a) and the corresponding GPA ε_{yy} strain map (b) of the bulk PBC.

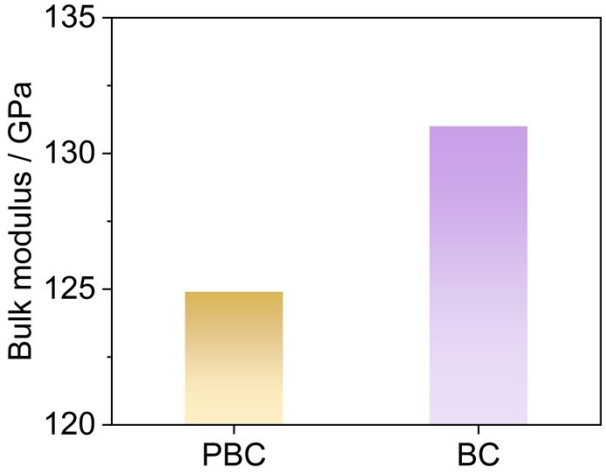

Fig. S4. Bulk modulus of PBC and B9C.

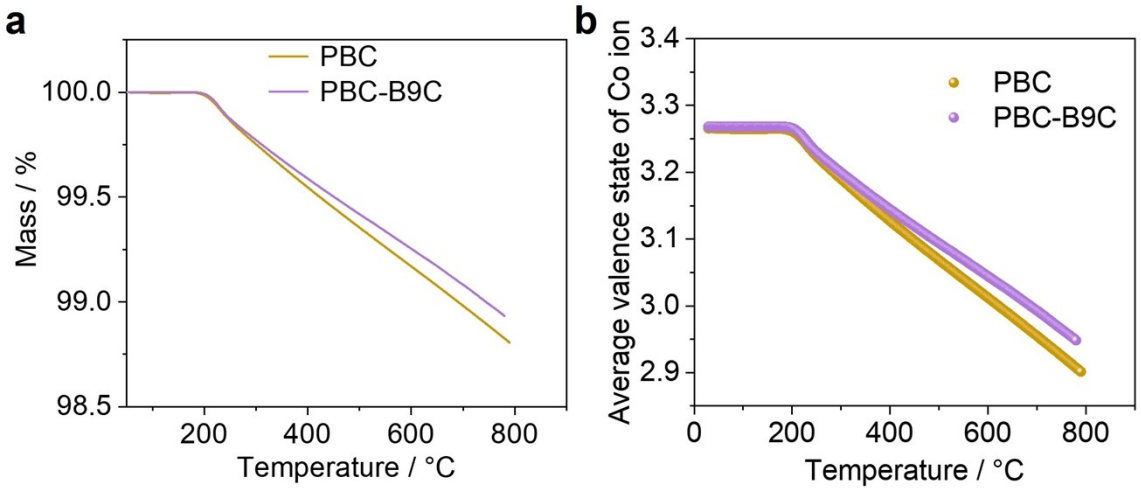

Fig. S5. Average valence state of Co ion of PBC-B9C and PBC samples measured in air in the temperature range of RT to 800 °C.

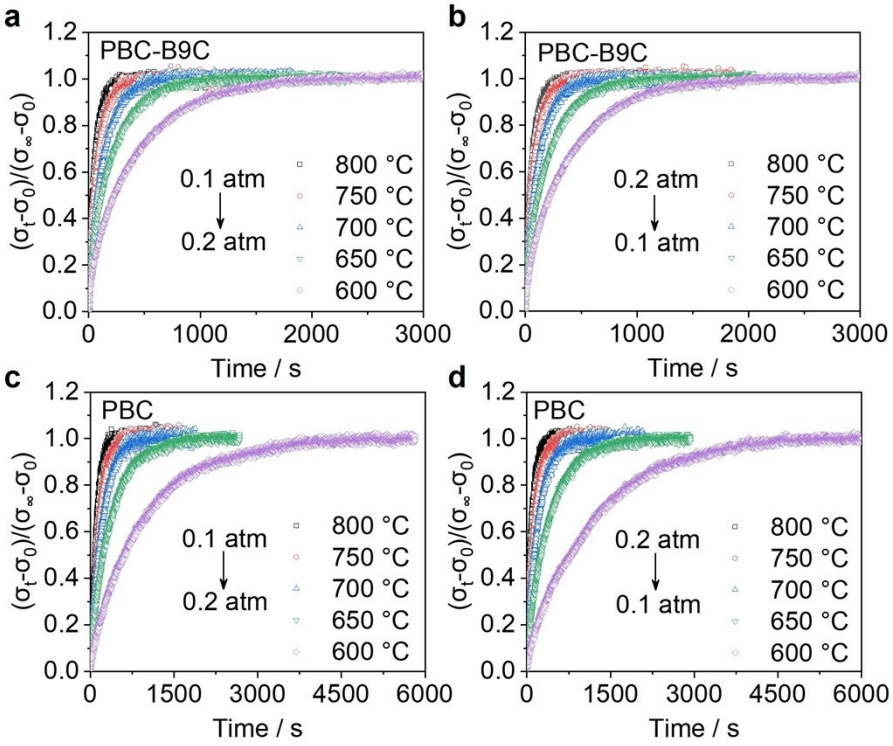

Fig. S6. ECR response curves of PBC-B9C sample in temperature range of 600–800 °C upon immediately shifting the oxygen partial pressure from 0.1 to 0.2 atm (a) and from 0.2 to 0.1 atm (b). ECR response curves of PBC sample in temperature range of 600–800 °C after immediately shifting the oxygen partial pressure from 0.1 to 0.2 atm (c) and from 0.2 to 0.1 atm (d).

Table S2. The k_{ex} values of PBC and PBC-B9C samples between 0.1 and 0.2 atm, unit cm s^{-1}.

T / °C	PBC		PBC-B9C	
	0.1 to 0.2 atm	0.2 to 0.1 atm	0.1 to 0.2 atm	0.2 to 0.1 atm
800	4.8×10^{-4}	5.9×10^{-4}	8.9×10^{-4}	8.4×10^{-4}
750	3.1×10^{-4}	3.8×10^{-4}	6.1×10^{-4}	6.1×10^{-4}
700	1.9×10^{-4}	2.2×10^{-4}	3.7×10^{-4}	4.0×10^{-4}
650	1.1×10^{-4}	1.1×10^{-4}	2.1×10^{-4}	2.2×10^{-4}
600	0.9×10^{-4}	0.4×10^{-4}	1.1×10^{-4}	1.1×10^{-4}

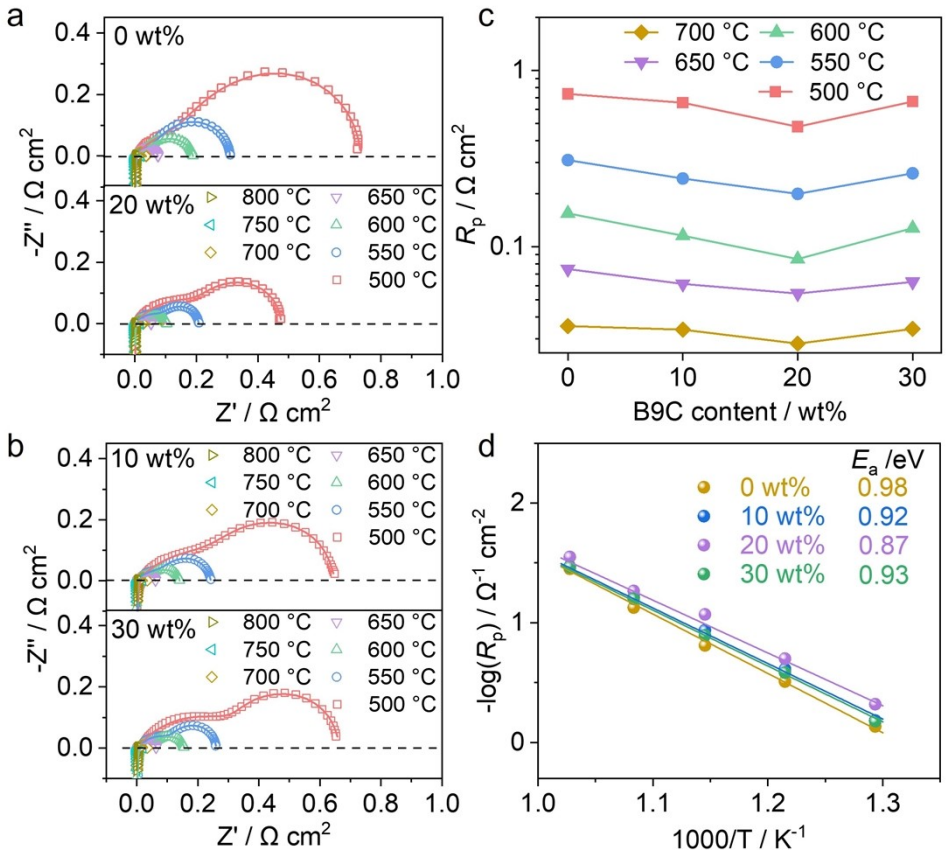

Fig. S7. EIS of PBC-*x* wt%B9C (x = 0, 10, 20, and 30) electrodes measured in air in temperature range of 500-800 °C (a, b). Fitted R_p of PBC-*x* wt%B9C (x = 0, 10, 20, and 30) electrodes (c). Arrhenius plots of R_p of PBC-*x* wt%B9C (x = 0, 10, 20, and 30) electrodes (d).

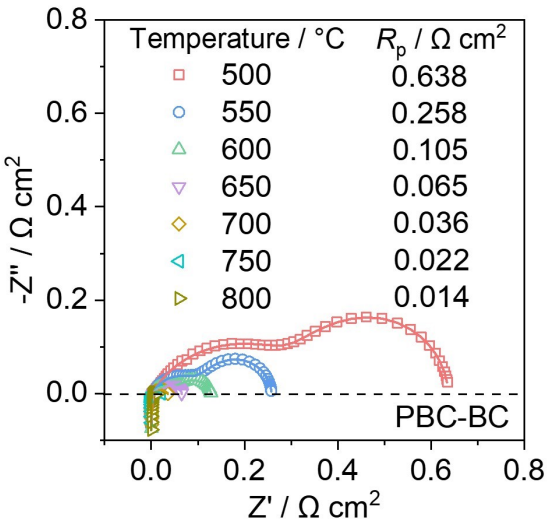

Fig. S8. EIS of PBC-BC electrode measured in air in temperature range of 550-800 °C.

Table S3. Fitted R_p values of elementary reactions of PBC-B9C and PBC electrodes measured at 650 °C under various oxygen partial pressures.

Oxygen partial	PBC-B9C / Ω cm^2				PBC / Ω cm^2			
pressure / atm	P1	P2	P3	P4	P1	P2	P3	P4
0.03	0.0346	0.0267	0.0096	0.0082	0.0324	0.0425	0.0065	0.0078
0.05	0.0211	0.0252	0.0090	0.0083	0.0196	0.0363	0.0065	0.0077
0.08	0.0130	0.0229	0.0090	0.0083	0.0121	0.0313	0.0063	0.0079
0.14	0.0070	0.0195	0.0093	0.0081	0.0065	0.0258	0.0061	0.0079
0.20	0.0046	0.0180	0.0090	0.0081	0.0044	0.0232	0.0061	0.0079
0.30	0.0021	0.0161	0.0090	0.0078	0.0022	0.0192	0.0072	0.0078
0.50	0.0012	0.0144	0.0083	0.0079	0.0011	0.0160	0.0073	0.0081
0.75	0.0006	0.0128	0.0088	0.0077	0.0005	0.0139	0.0074	0.0077
1	0.0004	0.0115	0.0087	0.0077	0.0004	0.0106	0.0087	0.0079

Table S4. Fitted R_p values of elementary reactions of PBC-B9C and PBC electrodes measured at different testing time at 700 °C.

Test time /	PBC-B9C			PBC		
h	LF	MF	HF	LF	MF	HF
12	0.0043	0.0124	0.0058	0.0048	0.0163	0.0053
108	0.0043	0.0132	0.0059	0.0048	0.0167	0.0055
216	0.0041	0.0140	0.0060	0.0049	0.0167	0.0057
408	0.0040	0.0149	0.0062	0.0049	0.0192	0.0057

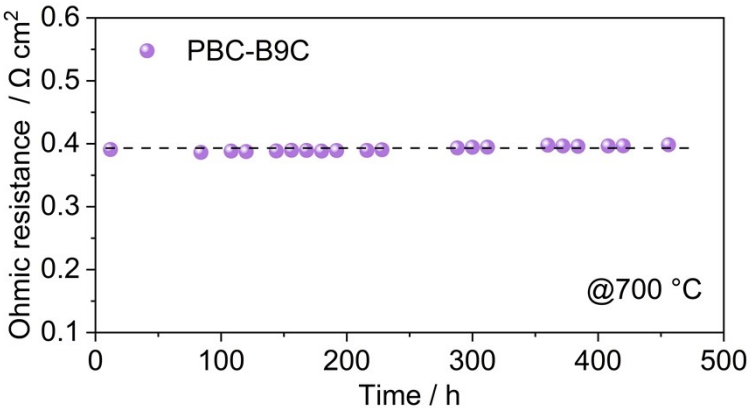

Fig. S9. Ohmic resistance change over testing time at 700 °C for PBC-B9C electrode in a LSGM-supported symmetric cell.

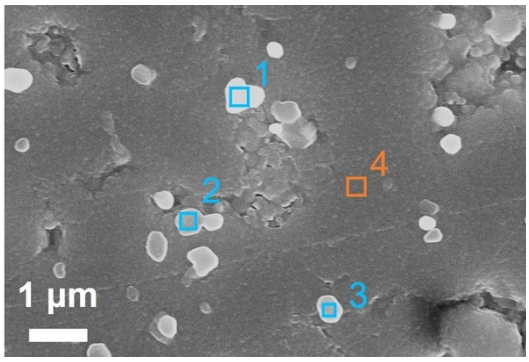

Fig. S10. SEM image of polished PBC pellet after treating at 800 °C for 100 h in air (marked area is selected for EDS analysis).

Table S5. Atomic percent of elements on area 1, 2, 3 and 4 in Fig. S10.

	O / %	Co / %	Ba / %	Pr / %	Ba/Pr
Area 1	60.21	19.61	14.49	5.69	2.54
Area 2	55.79	22.77	13.02	8.48	1.53
Area 3	56.29	22.15	13.68	7.89	1.73
Area 4	50.59	25.69	13.13	10.58	1.24

The high Ba/Pr atomic ratio of Areas 1-3 suggests that the bright small particles in Fig. S10 should be the segregated Ba-rich oxides.

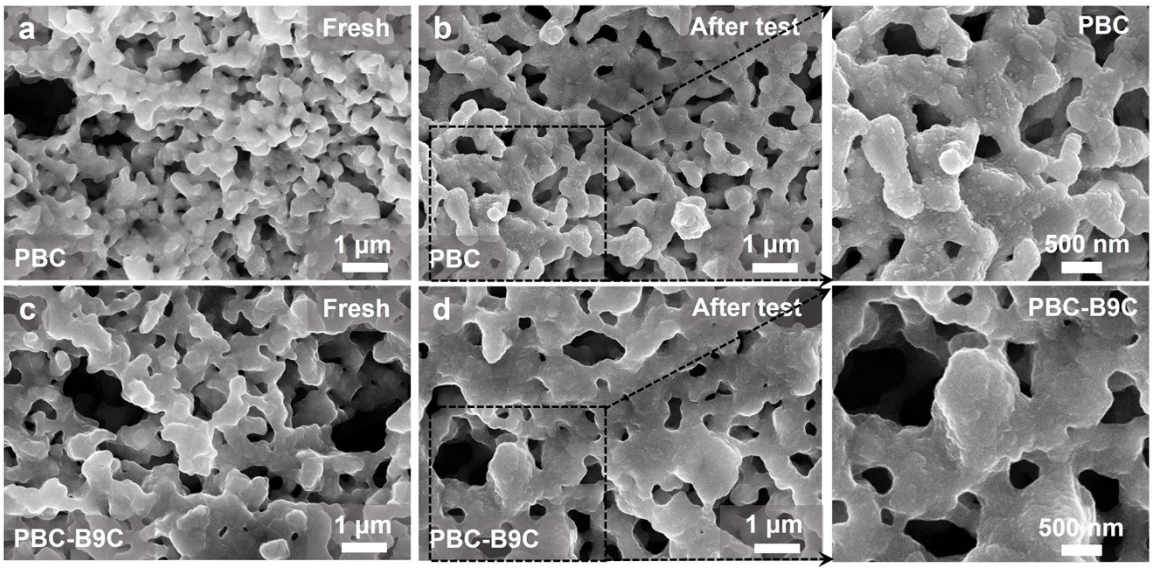

Fig. S11. SEM images of the electrode surface of PBC and PBC-B9C samples before test (a, c) and after 456 h test at 700 °C (b, d).

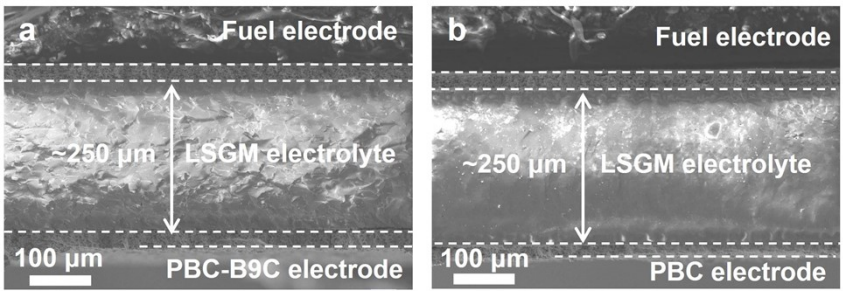

Fig. S12. Microstructure of the cross-section of Ni-GDC|LDC|LSGM|PBC-B9C (a) and Ni-GDC|LDC|LSGM|PBC (b) single cells.

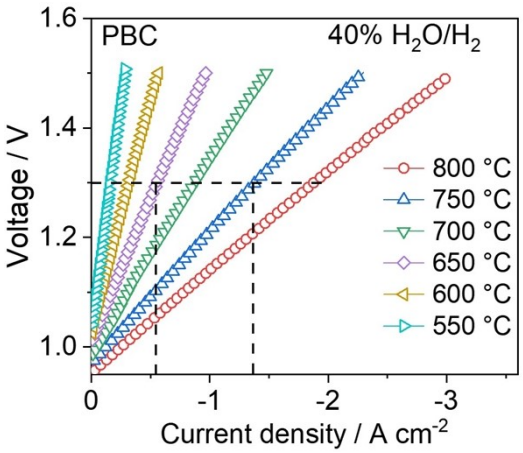

Fig. S13. I-V curves of PBC-based single cell in temperature range of 550-800 °C with 40% H_2O/H_2 at fuel side.